

Additional bounds on the pre Big–Bang–Nucleosynthesis Expansion by means of γ -rays from the Galactic Center

F. Donato

*Università degli Studi di Torino and
Istituto Nazionale di Fisica Nucleare, Sezione di Torino
via P. Giuria 1, I-10125 Torino, Italy
(donato@to.infn.it)*

N. Fornengo

*Università degli Studi di Torino and
Istituto Nazionale di Fisica Nucleare, Sezione di Torino
via P. Giuria 1, I-10125 Torino, Italy
(fornengo@to.infn.it)*

M. Schelke

*Istituto Nazionale di Fisica Nucleare, Sezione di Torino
via P. Giuria 1, I-10125 Torino, Italy
(schelke@to.infn.it)
(Dated: September 5, 2018)*

The possibility to use γ -ray data from the Galactic Center (GC) to constrain the cosmological evolution of the Universe in a phase prior to primordial nucleosynthesis, namely around the time of cold dark matter (CDM) decoupling, is analyzed. The basic idea is that in a modified cosmological scenario, where the Hubble expansion rate is enhanced with respect to the standard case, the CDM decoupling is anticipated and the relic abundance of a given dark matter (DM) candidate enhanced. This implies that the present amount of CDM in the Universe may be explained by a Weakly Interacting Massive Particle (WIMP) which possesses annihilation cross section (much) larger than in standard cosmology. This enhanced annihilation implies larger fluxes of indirect detection signals of CDM. We show that the HESS measurements can set bounds for WIMPs heavier than a few hundreds of GeV, depending on the actual DM halo profile. These results are complementary to those obtained in a previous analysis based on cosmic antiprotons. For a Moore DM profile, γ -ray data limit the maximal Hubble rate enhancement to be below a factor of 100. Moreover, a WIMP heavier than 1 TeV is not compatible with a cosmological scenario with enhanced expansion rate prior to Big Bang Nucleosynthesis (BBN). Less steep DM profiles provide less stringent bounds, depending of the cosmological scenario.

PACS numbers: 95.35.+d, 95.36.+x, 98.80.-k, 04.50.+h, 96.50.S-, 98.70.Sa, 98.80.Cq

I. INTRODUCTION

In a recent paper [1] we discussed the possibility to derive limits to the expansion rate of the Universe around the time when cold dark matter (CDM) decouples from the thermal bath, by using the fact that today these dark matter (DM) particles form the halo of our Galaxy and they may annihilate producing antiprotons. The measured antiproton flux has been shown to be compatible with the expected background originated by standard cosmic-ray spallation: this fact leads to the possibility to use antiprotons as a powerful tool for constraining DM properties (see *e.g.* Refs. [2, 3]). By assuming that DM is in the form of a generic Weakly Interacting Massive Particle (WIMP) candidate, we obtained relatively stringent bound on the Universe dynamics in a period

prior to the primordial nucleosynthesis phase (preBBN), which is not directly constrained by other observations. We showed that, despite the large uncertainties in the knowledge of the galactic propagation of antiprotons [2], bounds on the Hubble rate enhancement ranging from a factor of a few to a factor of 30 are present for DM masses lighter than 100 GeV, while for a mass of 500 GeV the bound falls in the range 50–500. These bounds loosen for heavier DM particles.

We remind here that the possibility to set a bound to the enhancement of the Hubble expansion rate in the early Universe by means of WIMP indirect detection signals relies on the fact that a larger Hubble rate induces an anticipated DM decoupling and an ensuing larger relic abundance, for a fixed annihilation cross section. This may happen, for instance, in scalar–tensor cosmology [4],

in quintessence models with a kination phase [5], and for anisotropic expansion and other models of modified expansion [6, 7].

When the decoupling is anticipated, a DM relic abundance able to explain the current observational data is obtained for larger DM annihilation cross sections, as compared to the standard cosmological case. This means that larger indirect detection signals (which are proportional to the DM annihilation cross section) are predicted: the larger the enhancement of the Hubble rate, the larger the indirect detection signal [4]. Comparison with experimental data reflects in limits on the DM possible Hubble rate enhancement. The actual results depend also on the specific cosmological model: in Ref. [1] we considered a general parametrization of the Hubble rate temperature dependence, and for definiteness we studied different classes of models: a Randall–Sundrum brane cosmology scenario [8], a kination scenario [5], a scalar–tensor cosmology scenario [4] and a simple case where the Hubble rate is just boosted by a constant factor. The same modellizations will be considered in the present study.

In this paper we extend our analysis by including also the possibility to use the data on γ -rays coming from the GC. DM particles may annihilate also to photons and the current experimental observations on the γ -ray flux, especially the ones coming from the GC where a large concentration of DM is expected, may be useful for our scope. With γ -rays we have to face the large uncertainty coming from the DM halo profile toward the GC, which is largely unknown. Nevertheless we will show that for typical DM halo profiles, bounds to the preBBN Hubble rate may be set.

The experimental data we will use are those from the GC obtained by the HESS [9, 10] and EGRET [11] telescopes. Since the HESS data refer to large energies (above few hundreds of GeV), we will be able to derive bounds for large-mass DM (above few hundreds of GeV): this nicely complements our previous results on antiprotons [1], which were quite stringent for low mass WIMPs, but loose for heavy ones. We will also show that EGRET data in the GeV region are able to set limits in the intermediate WIMP mass range (at least for the most steep DM profiles).

Our analysis will be independent of the specific DM candidate: the only assumption is that the WIMP we are considering is responsible for the observed DM amount [12]:

$$0.092 \leq \Omega_{\text{CDM}} h^2 \leq 0.124 \quad (1)$$

where Ω_{CDM} is the density parameter of CDM, and its annihilation cross section is dominantly temperature-independent (or s -wave). Deviations from this situation

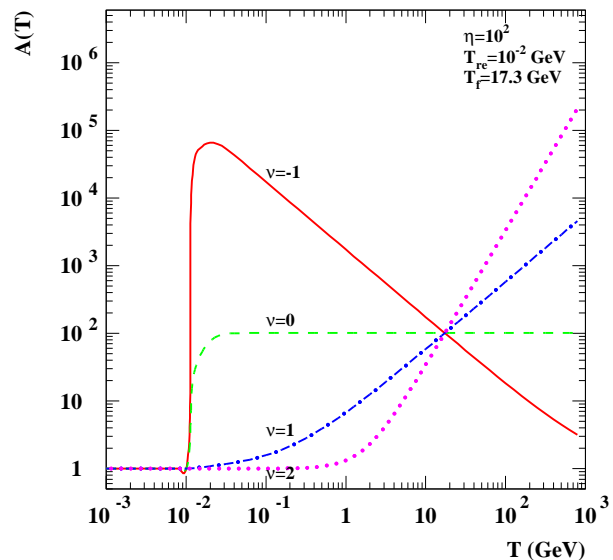


FIG. 1: Different models for the Hubble rate enhancement function $A(T)$, defined in Eq. (4). The Figure is taken from Ref. [1]. Notice that the evolution of the Universe runs from right to left. The solid (red) line has a slope parameter $\nu = -1$, the dashed (green) line $\nu = 0$, the dash-dotted (blue) $\nu = 1$ and the dotted (purple) line has $\nu = 2$. All curves refer to $\eta = 10^2$, $T_{\text{re}} = 10^{-2}$ GeV and $T_{\text{f}} = 17.3$ GeV (this freeze-out temperature refers, e.g., to a particle with mass of 500 GeV and annihilation cross section $\langle \sigma_{\text{ann}} v \rangle = 10^{-7}$ GeV $^{-2}$).

will lead to changes similar to those discussed in Ref. [1] for the antiproton case, to which we refer for additional discussion.

II. MODELS WITH INCREASED PRE-BBN EXPANSION

As mentioned in Sect. I, it is a common feature of some cosmological models to predict that the expansion rate $H(T)$ in the early Universe is larger than the Hubble expansion rate $H_{\text{GR}}(T)$ in standard cosmology. Quite generically, we may introduce a function $A(T)$ to quantify the enhancement of the Hubble rate:

$$H(T) = A(T)H_{\text{GR}}(T) \quad \text{at early times} \quad (2)$$

$$H(T) = H_{\text{GR}}(T) \quad \text{at later times.} \quad (3)$$

In Ref. [1] we introduced a parametrization of the enhancement function $A(T)$ which was shown to be applicable for important models like some scalar-tensor gravity models, some models with a kination phase and also some specific brane-world model. In this paper, we are going to consider the same parametrization, *i.e.*:

$$A(T) = 1 + \eta \left(\frac{T}{T_{\text{f}}} \right)^{\nu} \tanh \left(\frac{T - T_{\text{re}}}{T_{\text{re}}} \right) \quad (4)$$

for temperatures $T > T_{\text{re}}$ and $A(T) = 1$ for $T \leq T_{\text{re}}$. The enhancement function is shown in Fig. 1 for some specific parameter choices. The hyperbolic tangent serves to assure that $A(T)$ goes continuously to “1”, and $H \rightarrow H_{\text{GR}}$, before some “re-entering” temperature, T_{re} . We must require $T_{\text{re}} \gtrsim 1 \text{ MeV}$ to make sure not to be in conflict with the predictions of BBN and the formation of the Cosmic Microwave Background (CMB). For $T \gg T_{\text{re}}$ (and $\eta \gg 1$) we have approximately that:

$$A(T) \sim \eta \left(\frac{T}{T_{\text{f}}} \right)^\nu. \quad (5)$$

Thus, T_{f} is the normalization temperature at which $A(T_{\text{f}}) = \eta$. As in Ref. [1] we take T_{f} to be the temperature at which the WIMP DM candidate freezes out in standard cosmology. This means that η , as defined in our parametrization, is the enhancement of the Hubble rate at the time of the WIMP freeze-out. We will derive our results as bounds on η for different cosmological models, characterized by the temperature–evolutionary parameter ν : $\nu = 2$ refers to the Hubble rate evolution in a Randall–Sundrum type II brane cosmology scenario of Ref. [8]; $\nu = 1$ is the typical kination evolution, discussed *e.g.* in Ref. [5]; $\nu = -1$ is representative of the behavior found in scalar–tensor cosmology in Ref. [4]. The trivial case $\nu = 0$ refers to an overall boost of the Hubble rate.

For more details on the modified cosmological scenarios, the calculation of the relic abundance in these models, including some analytical results and discussion, we refer the reader to Ref. [1].

III. THE γ -RAY SIGNAL FROM THE GC

The most recent observations of the GC have been performed by the HESS Collaboration in the hundreds of GeV - few tens of TeV energy range. In Refs. [9, 10, 13] they have reported on the spectrum of very high energy γ -rays from a point-like source in the GC, with an unprecedented spatial resolution, going down to a solid angle of about 10^{-5} sr. The HESS spectrum of the central γ -ray source exhibits a clear power-law shape, with a spectral index of 2.2[9]-2.25[10]. Diffuse γ -ray emission extended along the galactic plane has been reported by the same Collaboration in Ref. [14]. The measured spectrum follows a power-law with spectral index near to 2.30 and has been shown to be compatible with a source of locally accelerated protons interacting with giant molecular clouds which are extended both in longitude and in latitude. This diffused component contributes to the central source only for a small fraction (10-15%) [10, 14]. The GC hosts more than one potential sources of γ -rays,

whose nature is still not clear. The most motivated astrophysical sources rely on particle acceleration near the supermassive black hole Sgr A* located at the center of our Galaxy, or in the region of the supernova remnant Sgr A. The γ radiation is produced from accelerated charged particles (mostly protons) interacting with the ambient matter or radiation. Another intriguing possibility resides in the γ -ray emission resulting from the annihilation of DM particles. Cosmological simulations of hierarchical structure formation predict a significant density cusp in the central parts of the galaxies. In that region annihilation of DM particles would be strongly enhanced, with extraordinary high expected fluxes for the annihilation products, such as γ -rays. The angular region explored by HESS is of the same order of the one of the probable black hole, or of the DM cusp.

We consider here a generic WIMP which composes the galactic DM. The flux $\Phi_\gamma(E_\gamma, \psi)$ of γ -rays of energy E_γ originated from the WIMP pair annihilation and coming from the angular direction ψ is given by:

$$\Phi_\gamma(E_\gamma, \psi) = \frac{1}{4\pi} \frac{\langle \sigma v \rangle_0}{m_\chi^2} \frac{dN_\gamma}{dE_\gamma} \frac{1}{2} I(\psi) \quad (6)$$

where $\langle \sigma v \rangle_0$ is the present annihilation cross section times the relative velocity averaged over the galactic velocity distribution function. dN_γ/dE_γ is the energy spectrum of γ -rays originated from a single WIMP pair annihilation and has been calculated by means of a Monte Carlo simulations with the PYTHIA package [15] as described in Ref. [16]. For definiteness, as we have done also for the antiproton analysis of Ref. [1], we are assuming the γ -ray energy spectrum originated by a $b\bar{b}$ quark pair. A different annihilation final state will not change substantially our results, much less than the astrophysical uncertainties.

The quantity $I(\psi)$ is the contribution of the squared DM density distribution along the line of sight (l.o.s.):

$$I(\psi) = \int_{\text{l.o.s.}} \rho^2(r(\lambda, \psi)) d\lambda(\psi). \quad (7)$$

Here ψ is the angle between the l.o.s. and the line pointing toward the GC ($\cos \psi = \cos l \cos b$, l and b being the galactic longitude and latitude, respectively). If Eq.(7) is used for comparison with experimental data, it must be averaged over the telescope observing angle $\Delta\psi$:

$$I_{\Delta\psi} = \frac{1}{\Delta\psi} \int_{\Delta\psi} I(\psi) d\psi. \quad (8)$$

The geometric factor $I(\psi)$ depends quadratically on the DM density profile and is very sensitive to its features, especially in the GC region where predictions

Isothermal	NFW	log-slope	$\alpha = 1.2$	Moore
18.9	6892	10229	98743	$7.7 \cdot 10^6$

TABLE I: Values for $I_{\Delta\psi}$ in Eq.(8) (in units of $\text{GeV}^2 \text{ cm}^{-6} \text{ kpc}$). See text for details.

for $\rho(\vec{r})$ differ mostly. The most common spherically-averaged density profiles can be parametrized as:

$$\rho(r) = \rho_l \left(\frac{R_\odot}{r} \right)^\gamma \left[\frac{1 + (R_\odot/a)^\alpha}{1 + (r/a)^\alpha} \right]^{(\beta-\gamma)/\alpha}, \quad (9)$$

where $r = |\vec{r}|$, $R_\odot = 8 \text{ kpc}$ is the distance of the Solar System from the GC along the galactic plane, a is a scale length and ρ_l is the total local (solar neighborhood) DM density. In particular, the isothermal, cored density profile is obtained with $(\alpha, \beta, \gamma) = (2, 2, 0)$, the Navarro, Frenk and White (NFW) profile [17] with $(\alpha, \beta, \gamma) = (1, 3, 1)$ and the Moore et al. profile [18] with $(\alpha, \beta, \gamma) = (1.5, 3, 1.5)$. We also consider a non-singular DM density distribution function derived from extensive numerical simulations, whose asymptotic regime is well fitted by a logarithmic slope [19]:

$$\rho(r) = \rho_{-2} \exp \left\{ -\frac{2}{\alpha} \left[\left(\frac{r}{r_{-2}} \right)^\alpha - 1 \right] \right\}, \quad (10)$$

where r_{-2} is the radius where the logarithmic slope is $\delta = -2$, and $\rho_{-2} \equiv \rho(r_{-2})$. The DM density predicted by these profiles at the GC (for very small r) varies so strongly that also the predicted DM signals may differ by several orders of magnitude. The profile as steep as 1.5 is disfavored by the most recent numerical simulations, which seem to indicate a power law index not exceeding 1.2 [20, 21]. We notice, however, that the experiments considered in this paper have a spatial resolution which is much narrower than the typical resolution size of numerical simulations. The simulated DM densities in the GCs are thus mere extrapolations. Moreover, we must be aware of the fact that the results from many rotational curves for galaxies of different morphological types are hardly explained by central DM cusps. Instead, they are more easily fitted by cored DM distributions, flattened towards the central region of the galaxy.

In Table I we show the values of the geometrical factor $I_{\Delta\psi}$ for the HESS telescope aperture ($\Delta\psi = 10^{-5} \text{ sr}$) and for various DM density profiles. The first column refers to an isothermal density distribution with a core $a = 3.5 \text{ kpc}$ and the second to a NFW with a scale length $a = 25 \text{ kpc}$. The third is for the log-slope of Eq. (10) with the parameters of the distribution G1 in Ref. [19]: $\alpha = 0.142$, $r_{-2} = 26.4 \text{ kpc}$ and $\rho_2 = 0.035 \text{ GeV cm}^{-3}$. The fourth column is the result for a profile obtained with $(\alpha, \beta, \gamma) = (1.2, 3, 1)$ with $a=25 \text{ kpc}$ [20, 21] and the last column refers to a Moore et al. profile with scale

length $a = 30 \text{ kpc}$. The value of ρ_l can be determined for each density profile requiring the compatibility with the measurements of rotational curves and the total mass of the Galaxy [22]. For definiteness, we have fixed $\rho_l = 0.3 \text{ GeV cm}^{-3}$ for all the density profiles in Table I. We notice that the parameter ρ_l enters as a mere scaling factor in Eq. 6: the effect of varying ρ_l is therefore easily taken into account.

IV. CONSTRAINING THE HUBBLE RATE WITH γ -RAYS

In order to derive the constraint on the enhancement of the Hubble rate, we first find the upper bound on $\langle \sigma v \rangle_0$ determined by the γ -ray observations, for any given halo profile.

Let us first explain our analysis for the HESS observation of high energy γ -rays from the GC. Here we have added the expected WIMP signal to a background that follows a power-law, $kE^{-\Gamma}$. The normalization and the index of the power-law are taken as free parameters. For each point in the grid-scan of (k, Γ) we find the maximum allowed value of $\langle \sigma v \rangle_0$, which we statistically define as the value of the cross section at which the reduced χ^2 equals 3. The reduced χ^2 is defined as:

$$\chi_{\text{red}}^2 = \frac{1}{N} \sum_{n=1}^D \left(\frac{\Phi_\chi(n) + \Phi_B(n) - \Phi_{\text{Obs}}(n)}{\sigma_{\text{Obs}}(n)} \right)^2 \quad (11)$$

where N is the number of degrees of freedom, $\Phi_\chi(n)$ is the expected WIMP flux, as calculated using Eq. (6), at the energy of the n -th data-point ($\Phi_\chi(n)$ obviously vanishes when $E_n \gtrsim m_\chi$). The background flux is assumed to be $\Phi_B(n) = kE_n^{-\Gamma}$, while the observed flux is $\Phi_{\text{Obs}}(n)$. The $1-\sigma$ error of the observation is denoted $\sigma_{\text{Obs}}(n)$. For the analysis, we use the 17 data points from the HESS 2003 observation of the GC [9, 13]. They cover the energy range $280 \text{ GeV} - 8.83 \text{ TeV}$. These data can therefore be used to constrain WIMP heavier than about 300 GeV (the annihilation process in the Galaxy occurs almost at rest: therefore there is a kinematic cut off at the WIMP mass for the γ -ray energy).

The χ^2 analysis, as described above, gives us the upper limit of the cross section for each point in the (k, Γ) grid for fixed WIMP mass and halo profile. Finally we extract the grid-point which gives the biggest value of the cross section. This upper bound on $\langle \sigma v \rangle_0$ is shown in Fig. 2, as

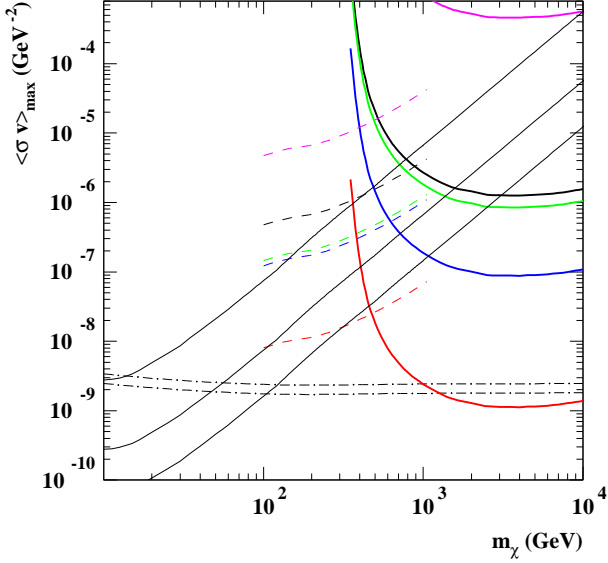


FIG. 2: Bounds on the WIMP annihilation cross section $\langle\sigma v\rangle_0$ as a function of the WIMP mass. The curved lines at large WIMP mass show the *upper* bounds derived from the HESS observation of γ -rays from the GC. The derivation has been made for five different DM halo profiles. From top to bottom these are: the isothermal model, the NFW model, the 'log' slope, a power-law slope with index 1.2, the Moore et al. profile (see text for more details). The dashed lines show analogous *upper* limits derived using the γ -ray data from the EGRET detector, for the same set of galactic halo models. The EGRET limits are plotted only in the mass interval which is relevant for the analysis of this paper. The slanted solid lines show the *upper* limits coming from the observations of cosmic antiprotons [1]. The central line refers to the best estimate for the antiproton DM signal. The upper and lower lines refer to the astrophysical uncertainties in the galactic propagation parameters [1, 2]. Finally, the horizontal dot-dashed lines shows the *lower* bound on the cross section as derived from the WIMP relic density constraint assuming the standard cosmological model and a temperature independent WIMP annihilation cross section.

a function of the WIMP mass for the five different halo profiles discussed above. As expected, the result depends strongly on the halo profile.

Before we continue to explain how the upper limit on the cross section was derived from other observational data, let us show some examples of the differential photon production which correspond to the upper limit on the WIMP annihilation cross section. In Fig. 3 we show the result for the NFW halo profile and for two different masses. The flux is calculated using Eq. (6) and inserting the upper bound on $\langle\sigma v\rangle_0$ for the given mass and halo profile. Also shown are the HESS 2003 observations of the GC as well as the fitted power-law background. Note that as the parameters of the back-

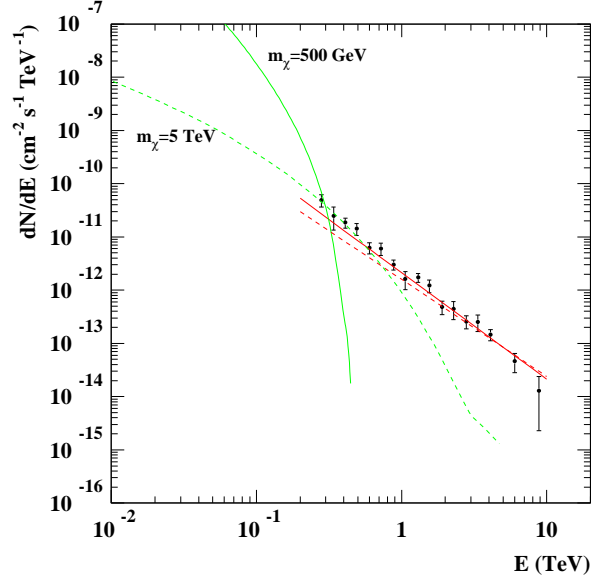


FIG. 3: γ -ray spectra as a function of energy. The data points refer to HESS [9, 13]. The solid and dashed (green) curves refer to the maximal allowable contribution to the γ -ray flux from WIMP annihilation: the cases of 500 GeV and 5 TeV WIMPs are plotted. The solid and dashed (red) straight lines refer to a standard-source power-law contribution to the HESS data, as obtained by our fit (see text for more details).

ground are treated as free parameters, they are different for the different WIMP masses and halo profiles. In the shown examples, the background parameters associated with the upper bound on the WIMP cross section are $(k, \Gamma) = (0.177 \cdot 10^{-6} \text{ cm}^{-2} \text{ s}^{-1} \text{ TeV}^{-1} \text{ sr}^{-1}, 2.00)$ and $(k, \Gamma) = (0.133 \cdot 10^{-6} \text{ cm}^{-2} \text{ s}^{-1} \text{ TeV}^{-1} \text{ sr}^{-1}, 1.83)$ for WIMP masses of 500 GeV and 5 TeV respectively.

Coming back to the limit on the WIMP annihilation cross section, Fig. 2 shows also the upper limit as derived from the EGRET. The EGRET data [11] span from energies of around 0.039 GeV to around 14.9 GeV with an angular resolution given by the longitude-latitude aperture: $|\Delta l| \leq 5^\circ$, $|\Delta b| \leq 2^\circ$. The geometric factor for the EGRET experiment has been taken from Ref. [16], for the same density distribution functions described in the previous Section. At these energies there is a γ -ray background from nucleonic reactions between cosmic rays and interstellar medium, electron bremsstrahlung and inverse Compton. We assume it to be the same as the one described in Ref. [16]. We apply the following analysis only for the two highest EGRET energy bins, i.e. $E_n \sim 6.2$ GeV and $E_n \sim 14.9$ GeV, which are the most constraining for the masses we are dealing with. For a given WIMP mass and halo profile we make a scan in the WIMP annihilation cross section to find its upper

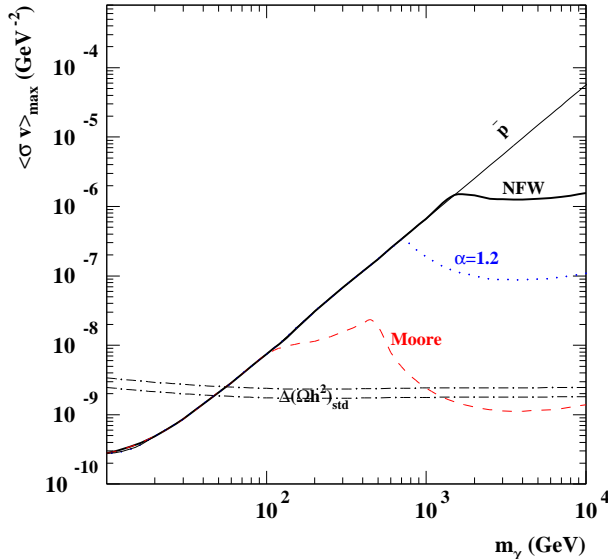


FIG. 4: Summary of the DM indirect detection limits on the WIMP annihilation cross section (for a temperature independent cross section). The allowed region lies above the horizontal dot-dashed lines (which refer to the relic density constraint) and below the slanted/curved lines, for any given DM density profile. The slanted part of the upper bound is due to cosmic antiprotons, while the curved part to γ -rays from the GC (from HESS data at large WIMP masses, EGRET at intermediate masses).

limit taken to be the 2σ bound:

$$\Phi_\chi(n) + \Phi_B(n) - \Phi_{\text{Obs}}(n) \leq 2\sigma_{\text{Obs}}(n) \quad (12)$$

The observational error, that we use, only includes the statistical error. We use the limit from the most constraining of the two data points. For the mass range relevant here, it is always the highest energy bin which provides the bound, except for a WIMP mass of 100 GeV. In Fig. 2 we show only the WIMP range where the EGRET data could be of importance for the analysis of this paper. Finally, Fig. 2 shows, as slanted solid lines, the upper limit on $\langle\sigma v\rangle_0$ derived in our previous analysis [1] of the observational data on cosmic antiprotons. The central line refers to the best estimate for the antiproton DM signal, *i.e.* when the best set of astrophysical parameters are used in the calculation of the diffusion processes for the galactic cosmic rays [2]. The upper and lower lines refer to the uncertainty band arising from astrophysical uncertainties in the galactic propagation parameters [1, 2]. The horizontal dot-dashed line denote instead the *lower* limit on the annihilation cross section derived from the cosmological bound on the WIMP relic density Eq. (1) in standard cosmology.

The analysis of Fig. 2 shows interesting properties. In addition to the already discussed bound on $\langle\sigma v\rangle_0$ from

antiprotons, which sizeably constrains the maximal allowable annihilation cross section, especially for WIMPs lighter than a few hundreds of GeV, we now also have the bounds coming from γ -rays from the GC, which instead are relevant for heavy WIMPs. This is a consequence of the fact that HESS data refer to an energy range from a few hundreds of GeV up to few TeV. The figure clearly shows that, in order to have bounds on $\langle\sigma v\rangle_0$, the signal must be quite sizeable and this is possible only for very steep DM profiles like the Moore and NFW ones. In the case of the Moore profile, we have a tension between the γ -rays HESS data and the cosmological limit even for standard cosmology (a situation analogous to the one already observed for the antiproton signal produced by light WIMPs [1, 3]). Should the DM profile be the Moore one, very little room would be allowed for $\langle\sigma v\rangle_0$. This bound would also imply a finite possible range for the WIMP mass: from 50–100 GeV to about 1 TeV (even for standard cosmology), as a combination of cosmological data on the amount of DM, the antiproton component of cosmic-rays and the γ -ray signal for the GC. Less steep profiles are clearly much less constraining, and the isothermal case is always ineffective, being always less relevant than the antiproton bound. We remind that since antiprotons diffuse in the Galaxy, their flux is only mildly dependent on the DM profile [2]: the antiproton bounds are therefore practically unaffected by the choice of different halo shapes.

A summary of the different bounds derived in our analysis is given in Fig. 4, where we combine the upper limits on the WIMP annihilation cross section from the observations of the cosmic antiprotons and of the GC γ -rays, as observed by both EGRET and HESS. For any mass and halo profile we take the bound which is most constraining. The combined upper limit can be seen in Fig. 4 for three halo profiles.

V. THE MAXIMAL ENHANCEMENT OF THE HUBBLE RATE

An increased Hubble rate in the early Universe would increase the relic density of a given WIMP as compared to the situation in standard cosmology. The increase of the relic density is due to an anticipated freeze-out of the WIMP, as the annihilation rate cannot keep up with the expansion rate as long as in the standard case. WIMPs which satisfy the density constraint of Eq. (1) in the modified scenario would thus be underabundant in standard cosmology. Because of the inverse proportionality between the WIMP relic density and annihilation cross section, the WIMPs which fulfill the density constraint in the modified cosmologies have larger cross section than

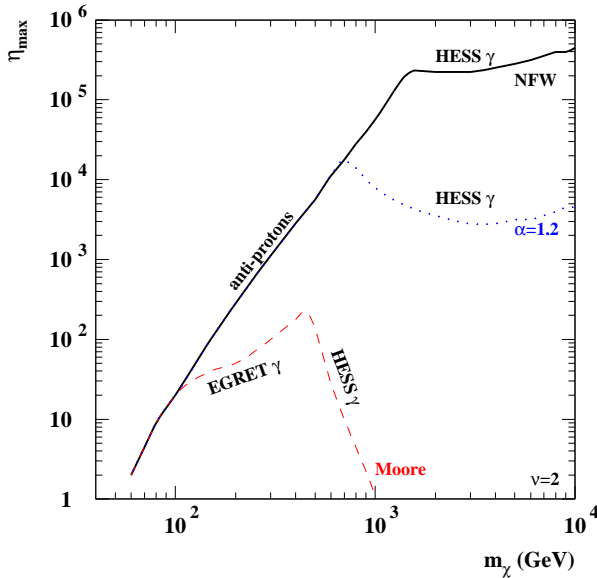


FIG. 5: Upper bound on the Hubble rate enhancement-parameter η . The bound is shown as a function of the WIMP mass and has been derived by combining the constraints on the WIMP relic density with the constraints derived from the observations of cosmic antiprotons and GC γ -rays. This figure shows the result for $T_{\text{re}} = 10^{-3}$ and $\nu = 2$ (RSII brane cosmology scenario [8]), where ν is defined in Eq. (4) for the Hubble rate enhancement function. We show the result for three different halo models. The labels on the curves show the origin of the bound.

those WIMPs which fulfill it in the standard case. The possible enhancement of the Hubble rate can therefore be constrained by applying at the same time the relic density constraint for the DM and the upper bound on the WIMP annihilation cross section as derived from the indirect searches for DM.

The argument above built on the crucial assumption that the WIMP annihilation cross section $\langle\sigma v\rangle$ is temperature independent. If this is not the case then the constraint from the indirect searches, which bound the present $\langle\sigma v\rangle_0$, could not be directly combined with the constraints on the relic density, which depends on the cross section in the early Universe. The relation between the cross section in the two epochs should be taken into account, a relation which would often lead to a looser bound on the enhancement of the Hubble rate. A discussion of this topic was given in Ref. [1], where it was shown that modifications are usually not very large, unless some specific situations, like *e.g.* coannihilation, occur. In this paper we will show our results only for the case where the WIMP annihilation cross section is temperature independent.

Let us derive the bound on the enhancement of the Hubble rate from the combination of the constraints on

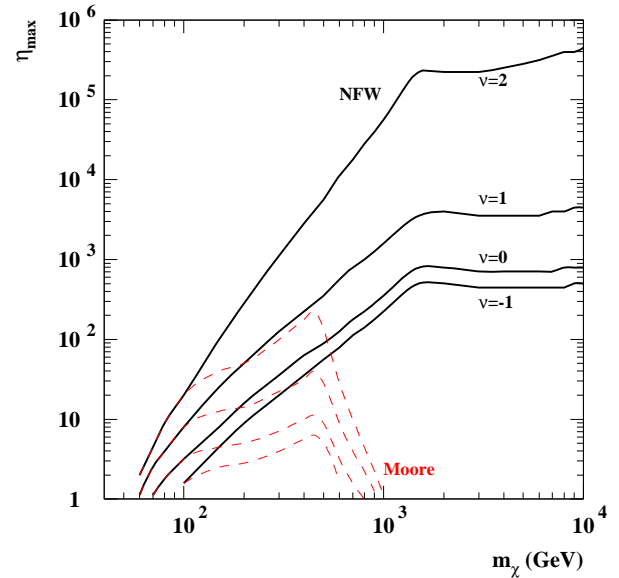


FIG. 6: The same as in Fig. 5, for different values of the parameter ν : $\nu = 2$ (RSII brane cosmology scenario [8]), $\nu = 1$ (kination scenario [5]), $\nu = 0$ and $\nu = -1$ (scalar-tensor cosmology scenario [4]). The NFW and Moore DM density profiles are shown.

the WIMP relic density and cross section. To obtain the WIMP relic density we solve the Boltzmann equation implemented with the modified Hubble function, Eq. (4). Let us therefore again go through the free parameters of the enhancement function. The freeze-out temperature, T_f , is determined by the WIMP mass and annihilation cross section and is therefore not a free parameter. The *re-entering* temperature, T_{re} , is a free parameter, but we showed in Ref. [1] that the bound on the Hubble expansion is independent of T_{re} as long as $T_{\text{re}} \ll T_f$. In this paper we set $T_{\text{re}} = 10^{-3}$ GeV, which is always much lower than the freeze-out temperature and which is the lowest value we can assume not to spoil BBN predictions. As we have mentioned earlier, the exponent ν in the enhancement function selects the kind of cosmological model. The only true free parameter is therefore η , which is normalized as the enhancement of the Hubble function at the time where the WIMP freezes out in standard cosmology.

To derive the upper bound on the parameter η we use for each WIMP mass and halo profile the upper bound on the annihilation cross section displayed in Fig. 4. For a given cosmological model, determined by the value of the ν parameter, the upper value of η is then found where the solution of the Boltzmann equation satisfies the upper bound of the density constraint Eq. (1). The upper bound on η as a function of the WIMP mass is shown in Fig. 5 for $\nu = 2$ and in Fig. 6 also for $\nu =$

$-1, 0, 1$. Knowing η , we can calculate the enhancement function $A(T)$ at any time once we choose a cosmological model.

Figs. 5 and 4 show that γ -ray data may be quite effective in constraining the preBBN Hubble rate for heavy WIMPs, and nicely complement in this large-mass range the antiproton results. In order to set bounds more stringent than antiprotons, however, a steep density profile is required: in the case of a NFW distribution, the γ -ray observations of HESS are able to set limits only for WIMPs heavier than 1 TeV. For this mass range, however, depending on the actual cosmological evolution, the bound can be relevant and much stronger than the antiproton bound: in the case of kination models, the γ -rays predicted for a NFW profile limits the maximal Hubble rate enhancement to be less than a factor of 5000; for scalar-tensor cosmologies the maximal enhancement goes down to a factor of 500. On the other hand, for a Moore profile the bounds are quite stringent: the maximal enhancement of the Hubble rate in this case is a factor of 100. In addition, for the Moore profile an enhancement is not possible for all the WIMP mass exceeding 1 TeV.

As an example of how our limits can be further used to constrain the basic properties of specific cosmological models, let us consider the implications for the brane Randall-Sundrum II model [8], which in our notations corresponds to $\nu = 2$ and $\eta = \sqrt{\rho_r(T_f)/(2\lambda)}$. Here ρ_r is the radiation energy density and λ is the tension of the brane, related to the 5-dimensional Planck mass M_5 by the relation $\lambda = \frac{3}{4\pi} \frac{M_5^6}{M_{\text{pl}}^2}$. For the Moore profile and WIMP masses $m_\chi = \mathcal{O}(500 \text{ GeV})$ we see from Fig. 5 that $\eta < \mathcal{O}(10^2)$. This implies $\lambda \gtrsim 2 \cdot 10^2 \text{ GeV}^4$, which corresponds to a lower bound on M_5 of $M_5 \gtrsim 7 \cdot 10^3 \text{ TeV}$. This is almost two orders of magnitude better than what was found in Ref. [1] by using antiproton data for the same value of WIMP mass. It is more stringent than what can be obtained from other cosmological tests: BBN sets the limit $M_5 > 13 \text{ TeV}$ [23, 24], while Ref. [25] sets $M_5 \gtrsim 600 \text{ TeV}$ but for a DM candidate in a specific supersymmetric model. Microgravity experiments [24] still set the best bound $M_5 > 10^5 \text{ TeV}$.

VI. CONCLUSIONS

In this paper we have discussed the possibility to use γ -ray data from the GC to constrain the cosmological evolution of the Universe in a phase prior to primordial nucleosynthesis, namely around the time of CDM decoupling from the primeval plasma. We extended the arguments already discussed in a previous paper of ours [1], where instead cosmic-ray antiprotons were used. The basic idea is that in a modified cosmological scenario, where

the Hubble expansion rate is enhanced with respect to the standard case, the CDM decoupling is anticipated and therefore the relic abundance of a given DM candidate is enhanced. This implies that the present amount of CDM in the Universe may be explained by a WIMP which possesses annihilation cross section (much) larger than in standard cosmology. This enhanced annihilation cross section implies larger fluxes of indirect detection signals of CDM, due to the annihilation of relic WIMPs in the halo of our Galaxy.

The stringent bounds on the maximal enhancement of the preBBN cosmic evolution, determined by the antiproton signal from DM annihilation and obtained in Ref. [1], have been complemented here by γ -ray searches. We have shown that the HESS measurements, which refer to relatively large γ -ray energies, are able to set constraints for WIMPs heavier than a few hundreds of GeV, depending on the actual DM halo profile. These results are complementary to those coming from antiprotons, which instead are important for WIMPs lighter than a few hundreds of GeV. In the case of a Moore profile, these bounds are very strong, and imply that a WIMP heavier than about 1 TeV is not compatible with a cosmological scenario with enhanced expansion rate prior to BBN. Less steep profiles provide less stringent bounds, always for heavy WIMPs: the NFW halo bounds the maximal Hubble rate enhancement to be below a factor between 5×10^2 and 5×10^5 , depending of the cosmological scenario. On the other hand, an isothermal sphere does not provide any relevant limit (better than the antiproton bound) for any mass. γ -ray data from the EGRET satellite are important for intermediate-mass WIMPs, but only for the very steep Moore profile.

Data from the GLAST satellite-based experiment will add relevant information for DM particles in a range of masses which goes from 100 GeV to a few hundreds of GeV, furtherly complementing the analysis we have been able to perform by using antiprotons (relevant for masses below 100-200 GeV) and available γ -rays from the GC (relevant for masses above about 500 GeV).

We can therefore conclude that DM indirect detection searches, in addition of being a powerful and important tool for studying the DM component of the Universe, may also have an important role in constraining the cosmic evolution, with an impact on dark energy models, modified gravity scenarios and theories of extra-dimensions.

Acknowledgments

We thank Prof. A. Bottino for stimulating and fruitful discussions. M.S. thanks P. Gondolo for useful and interesting comments. We acknowledge Research Grants

funded jointly by the Italian Ministero dell'Istruzione, dell'Università e della Ricerca (MIUR), by the University

of Torino and by the Istituto Nazionale di Fisica Nucleare (INFN) within the *Astroparticle Physics Project*.

-
- [1] Schelke M, Catena R, Fornengo N, Masiero A, Pietroni M, (2006) Phys. Rev. D **74** 083505.
 - [2] Donato F, Fornengo N, Maurin D, Salati P and Taillet R, (2004) Phys. Rev. D **69** 063501.
 - [3] A. Bottino, F. Donato, N. Fornengo, P. Salati, Phys. Rev. D **72** (2005) 083518.
 - [4] R. Catena, N. Fornengo, A. Masiero, M. Pietroni and F. Rosati, Phys. Rev. D **70**, 063519 (2004)
 - [5] P. Salati, Phys. Lett. B **571**, 121 (2003); F. Rosati, Phys. Lett. B **570**, 5 (2003); S. Profumo and P. Ullio, JCAP **0311**, 006 (2003); C. Pallis, JCAP **0510**, 015 (2005).
 - [6] J. D. Barrow, Nucl. Phys. B **208**, 501 (1982).
 - [7] M. Kamionkowski and M. S. Turner, Phys. Rev. D **42**, 3310 (1990).
 - [8] L. Randall and R. Sundrum, Phys. Rev. Lett. **83**, 4690 (1999).
 - [9] F. Aharonian *et al.* (HESS Collaboration), Astron.Astrophys. 425 (2004) L13-L17
 - [10] F. Aharonian *et al.* (HESS Collaboration), Phys. Rev. Lett. 97 (2006) 221102
 - [11] S.D. Hunter *et al.* (EGRET Collaboration), Astrophys. J. **481**, 205 (1997).
 - [12] Spergel, D N *et al.* (WMAP Collaboration), [arXiv:astro-ph/0603449], subm. Astrophys. J.
 - [13] Data points have been taken from the table on the Collaboration web site: <http://www.mpi-hd.mpg.de/hfm/HESS/HESS.html>
 - [14] F. Aharonian *et al.* (HESS Collaboration), Nature 439 (2006) 695.
 - [15] T. Sjöstrand, P. Eden, C. Friberg, L. Lonnblad, G. Miu, S. Mrenna and E. Norrbin, Comput. Phys. Commun. **135**, 238 (2001).
 - [16] A. Bottino, F. Donato, N. Fornengo, S. Scopel, Phys. Rev. **D70** (2004) 015005.
 - [17] J.F. Navarro, C.S. Frenk and S.D.M. White, Astrophys. J. **462**, 563 (1996).
 - [18] Moore B *et al.*, Mon. Not. Roy. Astron. Soc. **310**, 1147 (1999).
 - [19] Navarro J F *et al.*, (2004) MNRAS **349** 1039.
 - [20] Diemand J, Moore B, Stadel J, (2004) MNRAS **352** 535.
 - [21] Diemand J, Moore B, Stadel J, (2004) MNRAS **353** 624.
 - [22] P. Belli, R. Cerulli, N. Fornengo and S. Scopel, Phys. Rev. D **66**, 043503 (2002).
 - [23] Bratt, J D, Gault, A C, Scherrer, R J, and Walker, T P, (2002) Phys. Lett. **546** 19.
 - [24] R. Durrer, AIP Conf. Proc. **782**, 202 (2005) [arXiv:hep-th/0507006].
 - [25] Nihei, T, Okada, T, and Seto, O, (2005) Phys. Rev. **D71** 063535